

## Studies on the Electron Transfer Reaction Mechanism between NO<sub>2</sub> and NO<sub>2</sub><sup>-</sup> Complexes in the Gas Phase

by Z.Y. Zhou<sup>1,2\*</sup>, H.W. Gao<sup>1</sup>, A.P. Fu<sup>1</sup> and B.N. Du<sup>1</sup>

<sup>1</sup>Department of Chemistry, Qufu Normal University, Shandong, Qufu 273165, China

<sup>2</sup>State Key Laboratory of Crystal Materials, Shandong University, Shandong, Jinan 250100, China

(Received May 20th, 2003; revised manuscript August 13th, 2003)

The electron transfer (ET) reaction between NO<sub>2</sub> and NO<sub>2</sub><sup>-</sup> complexes in the gas phase is investigated by Density functional theory (DFT). The geometry optimization of the nitrogen dioxide complexes and the precursor state in the process of ET reaction was performed at 6-311+G\* basis set level. The nitrogen dioxide molecule separation distances computed using DFT method were found to agree with second order Moller-Plesset perturbation theory level (MP2) results. The 351.1 nm (3.532 eV) photoelectron spectrum of the nitrite anion (NO<sub>2</sub><sup>-</sup>) is obtained. For the precursor complex of NO<sub>2</sub>...NO<sub>2</sub><sup>-</sup>, eight reasonable geometries on the potential energy surface are considered with the most stable structure being T1-type. The activation barriers and the coupling matrix elements in the electron transfer process are also calculated for four different transition states. Results indicate that the structures and properties of the precursor complex directly affect the electron transfer reaction mechanism and rate. The reacting system in the T1-type structure has lower activation barriers and greater coupling matrix elements than those in other type of structures. It is indicated that the most possible path of the electron transfer is the collision of NO<sub>2</sub> and NO<sub>2</sub><sup>-</sup> to form the precursor complex with the T1-type structure, then the electron transfer and structure organization take place, the successor is obtained via the transition state with a Π<sub>g</sub><sup>2</sup>-conjugated system. Finally the product is attained.

**Key words:** density functional theory, electron transfer system, precursor complex

The ET reaction is an important fundamental chemical process and has become the focus on theoretical and experimental studies [1–3]. In experiments, the electron transfer rates of many hetero-exchange reactions containing the nitrogen dioxide (NO<sub>2</sub>) or the nitrogen dioxide anion (NO<sub>2</sub><sup>-</sup>) species, taking as the acceptor or the donor in electron transfer processes, have been extensively measured using various experimental methods. Theoretically, in order to investigate a reasonable dependence of the reaction rate on various factors, the reaction kinetic parameters, the mechanism of electron transfer and other reactions containing NO<sub>2</sub> or NO<sub>2</sub><sup>-</sup> as the acceptor or the donor have been encompassed by many studies, and some models have been established [4–6]. Some high quality treatments with electron correlation have been used to investigate the potential energy curves and the corresponding spectroscopic properties including excitation energies, dissociation energies, ionization potentials and electron affinities [7–9], and great progress has been made in characterizing these sys-

---

\*Author for correspondence; e-mail: zhengyu@qfnu.edu.cn

tems well. In particular, during recent years enormous progress has been made in the experimental study of the interaction in the gas-phase ionic clusters. These studies constitute very important and fundamental sources of information for understanding various structural and spectroscopic properties of the precursor complex in reaction processes and their effect on the chemical reactivity.

Over the last two decades, simple electron transfer theory provided by various researchers [10–14] has been extensively studied in both theoretical and experimental aspects, and has been applied to approaches to the electron transfer process kinetics. An important species in this theory is the precursor complex. The structure and relevant properties of this precursor complex affect directly on the electron transfer mechanism and the rate. However, this precursor complex is structurally unstable, and is not amenable to experimental observation. In the absence of available experimental data, *ab initio* and density functional theory (DFT) calculations has played an auxiliary role in providing relevant information and in helping to elucidate the fundamental aspects regarding this precursor complex and its structure reorganization in the activation process. In some respects, this electron–transfer precursor complex, in which only the electron population changes, provides more information to the theoreticians and the experimentalists than the stable molecules and other reaction intermediate species. The presence of this anion precursor complex necessitates the use of a more flexible basis set and high level theoretical method than the one used for neutral or simply charged systems [15].

The main purpose of the present work is to obtain a more complete understanding of the nature of the interaction in the  $\text{NO}_2 \dots \text{NO}_2^-$  complex. For this system, geometry optimization is performed at the self-consistent field (SCF) and the electron correlation levels using a fairly large basis set with two sets of polarization functions. Several possible structures and corresponding energy properties are compared, and a complete set of vibrational frequencies and charge populations are calculated.

## PRELIMINARY CONSIDERATION AND COMPUTATIONAL DETAILS

Geometrical optimizations and electronic structure calculations have been made at the Beckes three parameter hybrid method using the LYP correlation functional (B3LYP) method of density functional theory (DFT) with 6-311+G\* basis set [16,17]. All calculations are carried out using the Gaussian 98 package. According to the ET reaction between  $\text{NO}_2$  and  $\text{NO}_2^-$ ; eight possible structures in precursor state have been considered when two isolated species contact: The four planar structures (T1, T2, T3, T4) and the four sandwich structures (T5, T6, T7, T8) shown in Figure 1. The calculations are carried out for three stages of the reacting system. The first is the reactants separated at the infinite distance and the second is the stable precursor complex. The third is the system at the transition state.

For the precursor complex, eight structural forms are optimized using the following three steps: (i) Keeping the optimized geometries ( $r_a$  and  $r_b$ ) of  $\text{NO}_2$  and  $\text{NO}_2^-$ , the contact distance ( $r$ ) between two species is optimized. (ii) Fixing the optimized contact distance  $r$  and keeping the N–O distance of the molecular fragment  $\text{NO}_2$  equal to the optimized one in the isolated state, the N–O distance  $r_b$  of the molecular fragment  $\text{NO}_2^-$  is optimized and the result is  $r_b'$ ; (iii) Keeping just optimized contact distance  $r$  and  $r_b'$ , the N–O distance  $r_a$  of the molecular fragment N–O in the precursor complex is also optimized and the value is  $r_a'$ , then the geometry of the encounter complex can be defined by three parameters:  $r, r_a', r_b'$ . The transition state is defined as the saddle point along the seam of crossing between the two non-adiabatic potential

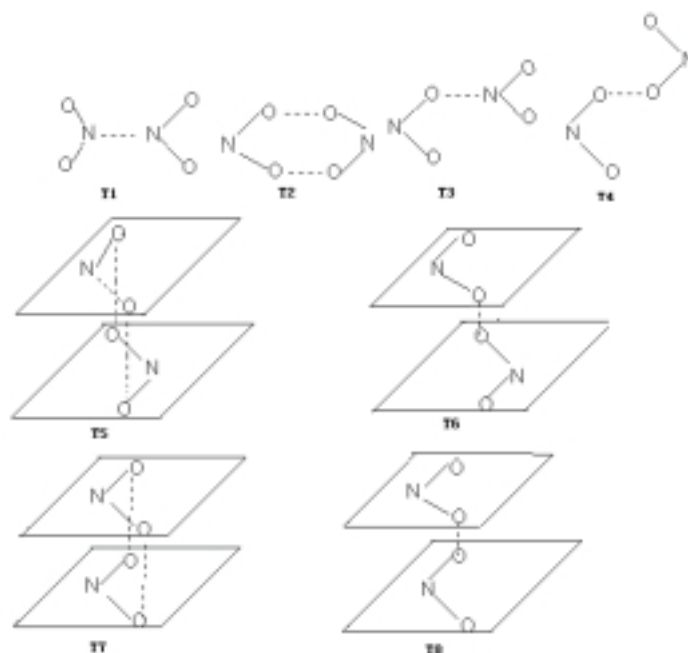
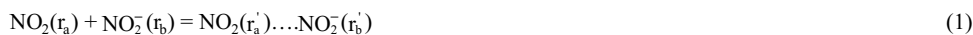


**Figure 1.** Eight possible structures in precursor state for the ET reaction between  $\text{NO}_2$  and  $\text{NO}_2^-$ .

energy surfaces corresponding to the initial and the final states of the electron transfer, respectively. In this study, we restrict our search of the transition state to the symmetric seam of energy surfaces. The symmetric transition state is obtained as the lowest energy point along this symmetric energy seam. In practice, this energy barrier may be alternatively determined *via* the following procedure, which is similar to the self-exchange model presented previously. For the thermal electron transfer case, the reactant system experiences a radiationless transition process, according to the self-exchange model, the  $\text{NO}_2$  and  $\text{NO}_2^-$  electron transfer may be expressed as

(i) forming of the precursor complex



(ii) reorganization of the precursor complex



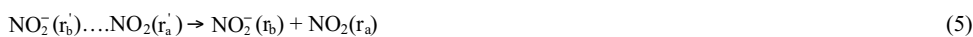
(iii) electron transfer



(iv) relaxation of the successor activated complex



(v) dissociation of the successor complex



Obviously, the energy change in Eq. (2) corresponds to the activation energy. At the activated state, the energy of the activated complex  $\text{NO}_2(r_a^*) \dots \text{NO}_2^-(r_b^*)$  before electron transfer is expressed as

$$E_i = E_{\text{NO}_2(r_a^*)} + E_{\text{NO}_2^-(r_b^*)} \quad (6)$$

After the electron transfer, the energy of this system becomes

$$E_f = E_{\text{NO}_2^-(r_a^*)} + E_{\text{NO}_2(r_b^*)} \quad (7)$$

where  $E_i(r^*)$  denotes the energy of the  $i$ th molecular fragment species in the reacting complex at the activated state  $[\text{NO}_2 \dots \text{NO}_2^-]$ . Energy conservation principle during the transition requires that  $E_f = E_i$ , thus

$$E_{\text{NO}_2(r_a^*)} + E_{\text{NO}_2^-(r_b^*)} = E_{\text{NO}_2^-(r_a^*)} + E_{\text{NO}_2(r_b^*)} \quad (8)$$

Since  $\text{NO}_2^-$  and  $\text{NO}_2$  are two systems with different properties, taking into account the Eq. (8), it can be deduced that  $r_a^*$  should be equal to  $r_b^*$ . Therefore, the energy of the system  $(\text{NO}_2 \dots \text{NO}_2^-)$  at the activated state is given by

$$E_a^* = E_{\text{NO}_2(r_a^*)} + E_{\text{NO}_2^-(r_a^*)} \quad (9)$$

Obviously Eq. (9) represents the energy curve formed in the crossing between the two non-adiabatic potential energy surfaces corresponding to the initial and the final states of the electron transfer, respectively. Minimization of Eq. (9) gives some relevant activation parameters. In view of the difficulty in expression the energy dependence on  $r_a^*$ , the energies of both molecular fragments for many  $r_a^*$  values, a range from 1.1933 Å ( $\text{NO}_2:r_c$ ) to 1.2579 Å ( $\text{NO}_2^-:r_c$ ), are alternatively calculated, and the numerical fitting analysis for this set of energy and  $r_a^*$  values can also easily give the optimized energy and  $r_a^*$  values at the transition state. The adiabatic activation energy ( $E_{ad}$ ) is easily obtained by subtracting the energy of each precursor complex from the corresponding energy at the activated state, *viz.*

$$E_{ad} = E_{\text{NO}_2 \dots \text{NO}_2^-(r_a^*, r_b^*)} - E_{\text{NO}_2 \dots \text{NO}_2^-(r_a', r_b')} \quad (10)$$

Actually this state intuitively represents the geometry, where electron transfer is likely to take place.

In addition, in order to test the effect of the electronic coupling interaction between the initial and the final states at the different molecular orientations on the activation energy of the electron transfer system  $(\text{NO}_2 \dots \text{NO}_2^-)$ , the non-adiabatic activation energy ( $E_d$ ) is then obtained by subtracting the energies of two isolated species ( $\text{NO}_2$  and  $\text{NO}_2^-$ ) at their own equilibrium geometries from the energy of the crossing point

$$E_d = E_{\text{NO}_2(r_a^*)} + E_{\text{NO}_2^-(r_b^*)} - E_{\text{NO}_2(r_a)} - E_{\text{NO}_2^-(r_b)} \quad (11)$$

Thus, the electronic couple matrix element or the energy reduction caused by the coupling between the initial and the final state of electron transfer may be obtained by

$$H_{if} = E_d - E_{ad} \quad (12)$$

## RESULTS AND DISCUSSION

*Optimized structures, energies and relevant spectroscopic properties.* Before the discussion on the structures of the precursor complex and the activation complex for the ET system, it is useful to test the applicability of *ab initio* calculation level to this system. The calculations on the isolated species,  $\text{NO}_2(\tilde{X}^2A_1)$  and  $\text{NO}_2^-(\tilde{X}^1A_1)$  are performed at the Becke three parameter hybrid method using the LYP correlation functional levels with 6-311+G\* basis set. The calculations on the isolated species,  $\text{NO}_2(\tilde{X}^2A_1)$  and  $\text{NO}_2^-(\tilde{X}^1A_1)$ , were performed at the level of Becke three parameter hybrid functional combined with the Lee, Yang and Parr correlation function,

(B3LYP), using the 6-311+G\* basis set. The optimized structures, energies and vibrational frequencies of NO<sub>2</sub> and NO<sub>2</sub><sup>-</sup> are summarized in Table 1. By comparing the calculated and experimental values for the spectroscopic constants, some trends in the dependence of the quality of the results on the level of the theory can be identified. It may be noted that, even at the MP2 level, larger deviations were found than with B3LYP method. The worst agreement between calculated and experimental results was found using HF/6-311+G\*. The inclusion of electron correlation correction may decrease the errors in the internuclear distances and bond angles. The HF/6-311+G\* is as same as the MP2/6-311+G\*, the results indicate that significant accuracy is achieved in the comparison with the experimental values. Comparison of the experimental  $r_e$  and a values with those calculated at the B3LYP/6-311+G\* level results in an error in bond distance of about 0.0494~0.632% and in bond angle of about 0.3892~0.6072%. The mean absolute deviations between non-NO and NO stretching frequencies of NO<sub>2</sub> species and the raw B3LYP, MP2 and HF results are 49.34, 313.70 and 202.03 cm<sup>-1</sup>, respectively; while those of NO<sub>2</sub><sup>-</sup> are 42.25, 75.51 and 230.47 cm<sup>-1</sup>, respectively. It indicates that the raw B3LYP calculations approximate the observed fundamental frequencies much better than the MP2 and HF results. Therefore, the high level of conformity between the observed and calculated spectral features indicates that B3LYP method is a more straightforward and practical approach to deduce the observed fundamental vibrational frequencies for many molecules whose vibrational spectra are not well understood. The analysis has fully confirmed that this electron correlation method is applicable in investigating the structure and spectroscopic properties of these small species containing nitrogen.

**Table 1.** Calculated bond distance, bond angle and spectroscopic properties for NO<sub>2</sub> and NO<sub>2</sub><sup>-</sup>.

Species	Method	$r_e$ (Å)	A	$\omega_e$ (cm <sup>-1</sup> )			ref
NO <sub>2</sub>	exp <sup>a</sup>	1.19389	133.857	$\omega_1^0 = 1325.33$	$\omega_2^0 = 750.14$	$\omega_3^0 = 1633.86$	1
	HF/6-311+G*	1.156	136.3935	$\omega_1^0 = 1604.4808$	$\omega_2^0 = 848.3366$	$\omega_3^0 = 1862.6093$	
	MP2/6-311+G*	1.2026	133.939	$\omega_1^0 = 1378.8469$	$\omega_2^0 = 772.9799$	$\omega_3^0 = 2498.6236$	
	B3LYP/6-311+G*	1.1933	134.378	$\omega_1^0 = 1391.1199$	$\omega_2^0 = 764.3676$	$\omega_3^0 = 1701.5807$	
NO <sub>2</sub> <sup>-</sup>	exp <sup>a</sup>	1.25	117.5	$\omega_1^0 = 1284$	$\omega_2^0 = 776$	$\omega_3^0 = 1244$	2
	HF/6-311+G*	1.2192	117.4233	$\omega_1^0 = 1575.2652$	$\omega_2^0 = 900.6980$	$\omega_3^0 = 1519.4456$	
	MP2/6-311+G*	1.2643	116.3184	$\omega_1^0 = 1401.0708$	$\omega_2^0 = 802.7566$	$\omega_3^0 = 1326.6978$	
	B3LYP/6-311+G*	1.2579	116.7865	$\omega_1^0 = 1334.1717$	$\omega_2^0 = 799.2854$	$\omega_3^0 = 1297.2803$	

<sup>a</sup>data from Ref. 3.

*Precursor complexes and transition state.* Formation of the precursor complex from the isolated redox species is the first stage of the ET reaction. The geometrical configuration of the precursor complex influences directly not only on the activation energy of reaction but also on the electron transfer coupling matrix element and further the electron transfer rate. Thus it is very important to find various possible geometrical configurations for the precursor complex. According to the ET reaction between  $\text{NO}_2$  and  $\text{NO}_2^-$ , eight possible structures in precursor state have been considered when two isolated species contact: four planar structures (T1, T2, T3, T4) and four sandwich structures (T5, T6, T7, T8) (shown in Figure 1). According to the structures in Figure 1, the geometry optimization was performed. The results show that there is no stable position with the distance of the center of two-molecule decreasing for T5, T6, T7 and T8. That is to say, the potential energy curve *versus* the reaction coordinate has no minimum point, so the conclusion can be derived that no stable equilibrium geometry for these four orientations is existed. Actually, from the analysis of the key orbital of the species  $\text{NO}_2$  and  $\text{NO}_2^-$ , structure T1, T2, T3, T4 is preferred because the overlap between the electron acceptor orbital (mainly the outer shell  $\Pi_3^*$  of  $\text{NO}_2$ ) and the electron donor orbital (mainly the outer shell  $\Pi_4^*$  of  $\text{NO}_2^-$ ) will be the largest. For simplicity, the later discussion will restrict to structure T1, T2, T3, T4. In the reacting system of T1, a new  $\sigma$  bond formed between two N atoms through the  $\text{SP}^2$  electrons. At the same time, there have a  $\Pi_6^0$ -conjugated system. T1-type activated state have a low activation barrier ( $E_a = 3.9215 \text{ kJ/mol}$ ) and a large coupling matrix element ( $H_{if} = 424.5951 \text{ cm}^{-1}$ ). For T3-type structure, the way to connect  $\text{NO}_2$  and  $\text{NO}_2^-$  species is through a N–O bond ( $\text{O}_2\text{N–ONO}$ ), which has similar characters with N–N bond in T1-type structure. Since the repulsive effect of the  $\sigma$ -lone pairs in the  $\text{sp}^2$  hybridization orbital of atom, the activation barrier for the T3-type transition state should be a slightly higher than that for the T1-type structure. For T2 and T4 type structures, two species were connected through the weak O–O bond ( $\text{ONO–ONO}$ ), for the T4-type, there have a  $\Pi_6^0$ -conjugated system, since the repulsive effect of two  $\sigma$ -lone pairs on the precursor complexes, the activation barrier is higher than that for T3-type structure (N–O bond). For the T2-type, there have a  $\Pi_6^{11}$ -conjugated system, since there have more anti-bond electrons and the repulsive effect of four  $\sigma$ -lone pairs, it can be expected the coupling interaction should be the smallest and have a highest activation barrier. For  $\text{NO}_2 \dots \text{NO}_2^-$  precursor complex in four different contact forms, the corresponding energies and other structural properties are summarized in Table 2.

In order to compare the stabilization of the precursor complex, the bonding energy between acceptor and donor is derived by

$$\Delta E = E_{\text{NO}_2} + E_{\text{NO}_2^-} - E_{\text{ps}} \quad (13)$$

where  $\Delta E$  is the bonding energy of the precursor complexes,  $E_{\text{ps}}$  is the energy of the precursor,  $E_{\text{NO}_2}$  and  $E_{\text{NO}_2^-}$  are the energy of the  $\text{NO}_2$  and  $\text{NO}_2^-$ , respectively. The larger the values of  $\Delta E$ , the more stable are the complexes. The results in Table 2 indicate

that the contact distances  $r_c$  between  $\text{NO}_2$  and  $\text{NO}_2^-$  in the precursor complexes are in range from 2.63 to 3.14 Å, which yields the binding energies of about 0.55–0.80 eV, and  $\Delta E$  decreased by the order of T1 > T3 > T4 > T2. For precursor complexes of T1-type structure, the bond length of one fragment is slightly longer than that of the isolated  $\text{NO}_2$  molecule, while the other  $\text{NO}_2$  fragment has the bond length very close to that of the isolated  $\text{NO}_2^-$  molecule. This observation indicates that the excess electron is well localized on the latter  $\text{NO}_2$  molecular fragment. The net charge populations also support this analysis. It indicates that the conjugated molecule is formed in the precursor complexes.

**Table 2.** The geometrical parameters, relevant energies and the coupling matrix elements for the reacting system,  $\text{NO}_2 + \text{NO}_2^-$ , in the precursor complex and the transition state at B3LYP/6-311+g\* level.

Species	T1	T2	T3	T4
Coupling state	A1	B2	A'	A'
Precursor complex				
$r(\text{Å})$	2.6287	3.1018	3.1445	2.8411
$r_0(\text{Å})$	1.2235	1.225	1.2279	1.2283
$r_c(\text{Å})$	1.2351	1.2387	1.2357	1.2287
$a_0(\text{Deg})$	124.0532	124.568	124.1161	123.7379
$a_c(\text{Deg})$	121.3448	120.9849	121.098	123.7374
$\Delta E(\text{eV})$	0.8047	0.5503	0.6160	0.5765
Transition complex				
$r_0 = r_c(\text{Å})$	1.2256	1.2279	1.2221	1.2283
$a_0 = a_c(\text{Deg})$	123.5442	123.7484	122.235	123.7379
$E_a(\text{kJ/mol})$	3.9215	4.6078	4.2453	4.4352
$H_{if}(\text{cm}^{-1})$	424.5951	220.9010	307.6373	260.3041

For the transition state the activation barrier corresponding precursor complex  $\text{NO}_2 \dots \text{NO}_2^-$  are 3.9215(T1), 4.6078(T2), 4.2453(T3) and 4.4352(T4) kJ/mol, respectively. The coupling matrix element referring to the difference between the activation energy and the energy of the system at the crossing point are 424.5951(T1), 220.9091(T2), 307.6373(T3) and 260.3041(T4)  $\text{cm}^{-1}$  for the four transition states, respectively. The most stable is the T1-type transition state with  $D_{2h}$  symmetry; the coupling matrix element is the largest (424.5951  $\text{cm}^{-1}$ ). The most unstable is the T2-type structure transition state. This phenomenon may be explained in terms of the orbital overlap interaction between the donor and the acceptor to form a  $\Pi_6^0$ -conjugated system. It is favorable with an effective overlap due to the orbital phase symmetry of both species,  $\text{NO}_2$  and  $\text{NO}_2^-$  and can be expected that the smaller contact distance may result in a larger overlap. For the T1-type structure, the  $\text{NO}_2$  species with a longer bond length is localized along the principle axis ( $D_2$  axis), and the  $\text{NO}_2^-$  species with a shorter bond length crosses the principal axis. This location of the two species,  $\text{NO}_2$  and  $\text{NO}_2^-$ , not only decreases the nuclear repulsion interaction, but also increases the orbital overlap between the donor ( $\text{NO}_2^-$ ) and the acceptor ( $\text{NO}_2$ ), thus the T1-type ac-

tivated state should have the lowest activation barrier (3.9215 kJ/mol) and the largest coupling matrix element ( $H_{if} = 424.5951 \text{ cm}^{-1}$ ).

According to previous discussion it seems more probable that the electron transfer in the  $\text{NO}_2 \dots \text{NO}_2^-$  system is more efficiently *via* a T1 precursor complex to form a  $\Pi_6^0$ -conjugated system, then to take place electron transfer and the structure reorganization and to obtain the transition state, through the transition state to form successor complex and finally to obtain product.

In conclusion, the structures and the properties of  $\text{NO}_2 + \text{NO}_2^-$  electron transfer system are studied in this paper at the B3LYP/6-311+G\* basis set level for the eight selected structures (shown in Figure 1). For the precursor complex of  $\text{NO}_2 \dots \text{NO}_2^-$ , the stability is compared through the bonding energy  $\Delta E$  of the precursor complexes with the T1-type is the most stable structure. The activation barriers and the coupling matrix elements in the electron transfer process are also calculated for four different transition states. Results indicate that the structures and properties of the precursor complex directly affect the electron transfer reaction mechanism. The reacting system in the T1-type structure has lower activation barriers and greater coupling matrix elements than those in other type structure. It is indicate that the most possible path of the electron transfer is the collision of  $\text{NO}_2$  and  $\text{NO}_2^-$  to form the precursor complex with the T1-type structure, then the electron transfer and structure organization are taken place, the successor is obtained *via* the transition state with a  $\Pi_6^0$ -conjugated system. Finally the product is attained.

#### Acknowledgment

This work was supported by the Natural Science Foundation of Shandong Province (Z2002F01), the National Key Laboratory Foundation of Crystal Material and the National Natural Science Foundation of China (2967305).

#### REFERENCES

1. Lafferty W.J. and Sams R.L., *J. Mol. Spectr.*, **66**, 478 (1977).
2. Jacox M.E., *J. Phys. Chem. Ref. Data*, **18**, 945 (1984).
3. Ervin K.M., Ho J. and Lineberger W.C., *J. Phys. Chem.*, **92**, 5405 (1988).
4. Becker C.H., *J. Chem. Phys.*, **76**, 5928 (1982).
5. Ohta K. and Morokuma K., *J. Phys. Chem.*, **91**, 401 (1987).
6. Vincent M.A. and Hillier I.H., *J. Phys. Chem.*, **99**, 3109 (1995).
7. Stratmann R.E. and Lucchese R.R., *J. Chem. Phys.*, **102**, 8493 (1995).
8. Clementi E. and Hofmann D.W.M., *J. Mol. Struct. (Theochem)*, **330**, 17 (1995).
9. Chandrasekher C.A., Griffith K.S. and Gellene G.I., *Int. J. Quantum Chem.*, **58**, 29 (1996).
10. Marcus R.A. and Sutin N., *Biochim. Biophys. Acta*, **811**, 265 (1985).
11. Hush N.S., *Trans. Faraday Soc.*, **57**, 557 (1961); *Electrochim. Acta*, **13**, 1005 (1968).
12. Sutin N., *Ann. Rev. Nucl. Soc.*, **57**, 155 (1965).
13. Newton M.D., *Int. J. Quantum Chem., Quantum Chem. Symp.*, **14**, 363 (1980).
14. Zhou Z.Y., Du B.N., Gao H.W. and Zhang W.C., *J. Mol. Struct. (Theochem)*, **548**, 53 (2001).
15. Zhou Z.Y., Chen G., Zhou X.M. and Fu H., *Int. J. Quantum Chem.*, **87**, 49 (2002).
16. Becke D., *Phys. Rev.*, **A38**, 3098 (1988).
17. Lee C., Yang W. and Parr R.G., *Phys. Rev.*, **B37**, 785 (1988).